Supplementary Information for

A robust thorium-organic framework as a bifunctional platform for iodine adsorption and Cr(VI) sensitization

Yiran Fu,[a, c] Xue Wang,[a] Yu Ju,[a] Zhaofa Zheng,[a,c] Jie Jian,[b] Zi-Jian Li,[a,c,*] Chan Jin,[a,c] Jian-Qiang Wang,[a,c,*] and Jian Lin[b,*]

[a] Shanghai Institute of Applied Physics, Chinese Academy of Sciences, 2019 Jia Luo Road, Shanghai 201800, P. R. China.

Email: lizijian@sinap.ac.cn; wangjianqiang@sinap.ac.cn

[b] School of Nuclear Science and Technology, Xi'an Jiaotong University, Xi'an, 710049, P. R. China. Email: linjian@xjtu.edu.cn

[c] University of Chinese Academy of Sciences, No.19(A) Yuquan Road, Shijingshan District, Beijing 100049, P. R. China

S1. EXPERIMENTAL SECTION

S1.1 Synthesis

Reagents. All reagents were purchased from chemical reagent suppliers and used without further purification. N,N-dimethylformamide (DMF, 99%), iodine (I_2, 99%), tetrahydrofuran (THF, 99.5%), $Al(NO_3)_3·9H_2O$ (99.99%), and $NaHCO_3$ (99%) were provided by Adamas. Na_2SO_4 (99.0%), NaF (99%), NaI (99%), NaBr (99%) and NaCl (99.5%) were purchased from Gre-agent. CH_3COOH (99%), ethanol (99.7%), acetone (99.5%), KNO_3 (99%), $Ca(NO_3)_2·4H_2O$ (99%), $Sr(NO_3)_2$ (99%), $Zn(NO_3)_2·6H_2O$ (99%), $Mg(NO_3)_2·6H_2O$ (99%), and $Na_3BO_3·9H_2O$ (99%) were provided by Sinopharm Chemical Reagent Co., Ltd. $Th(NO_3)_4·6H_2O$ (99%) was provided by Changchun Institute of Applied Chemistry, Chinese Academy of Sciences. Tris((4-carboxyl)phenylduryl)amine (98%) was provided by Jilin Chinese Academy of Sciences – Yanshen Technology Co., Ltd.

Synthesis. $Th(NO_3)_4·6H_2O$ (2.4 mg, 0.004 mmol), H_3TCBPA (5.2 mg, 0.0086 mmol), CH_3COOH (0.1 mL), H_2O (0.03 mL), and N, N-dimethylformamide (0.3 mL) were loaded in a 7 mL glass vial and heated at 120 °C for 48 h. Dark yellow crystals of **Th-TCBPA** were filtered, washed with DMF, and dried at room temperature. Anal. Calcd for $C_{196}H_{248}N_{18}Th_6O_{81}$, C, 42.46%; H, 4.51%; N, 4.55%. Found: C, 2.86%; H, 4.57%; N, 4.14%. IR: 3030(vw), 2177(vw), 2040(w), 1653(w), 1591(w), 1490(w), 1398(m), 1321(w), 1279(w), 1189(w), 1093(w), 1005(w), 830(w), 783(m), 725(w), 706(w), 652(w), 575(m), 547(w), 522(w), 501(w), 487(w), 442(w), 432(w), 427(w), 422(w), 417(m).

S1.2 Characterizations

X-ray Crystallography. Single-crystal X-ray diffraction data was collected on a Bruker D8-Venture single crystal X-ray diffractometer equipped with an IμS 3.0 microfocus X-ray source (Mo–Kα radiation, λ = 0.71073Å) and a CMOS detector. The data frames were collected using the APEX3 program and processed using the *SAINT* routine. The empirical absorption correction was applied using the SADABS program [1]. The structure was solved by Intrinsic Phasing with *ShelXT* [2] and refined with ShelXL [3] using *OLEX2* [4]. All the non-H atoms were subjected to anisotropic refinement by full-matrix program. Contributions to scattering due to these highly disordered solvent molecules were removed using the *SQUEEZE* routine of *PLATON* [5]. Structures were then refined again using the data generated. Crystal data and details of the data collection are given in Table S1. Powder X-ray diffraction (PXRD) data were collected on were collected from 2 to 40° with a step of 0.02° on a Bruker D8 Advance diffractometer with Cu Kα radiation (λ = 1.54178 Å). The calculated PXRD pattern was produced from the CIFs using the Mercury 1.4.2 program.

N_2 absorption and Brunauer-Emmett-Teller (BET) Analysis. The N_2 adsorption isotherms were recorded at 77 K by using a micromeritics ASAP 2020 surface area and porosity analyser. Before the adsorption measurements, the freshly prepared sample of **Th-TCBPA** was first exchange with DCM for 15 minutes three times and with n-hexane for 15 minutes three times. Then, the samples were activated with the "degas" port under the vacuum at 30°C for 3 h.

Thermogravimetric Analysis (TGA). TGA was carried out in an N_2 atmosphere with a heating rate of 10 °C/min from 40 °C to 800 °C on a NETZSCH STA 449 F3 Jupiter instrument. TGA indicated that the solvent species were removed gradually from room temperature in all cases.

X-ray photoelectron spectroscopy (XPS). The XPS data of iodine adsorbed samples were recorded on a Thermo Scientific ESCALAB 250Xi using monochromatic Al Kα (1486.8 eV) X-ray source with a spot size of 500 μm. The anode was operated at 15 kV and 10 mA.

Raman Spectroscopy. Raman spectra of **Th-TCBPA** samples were collected on a Renishaw inVia Raman Microscope with an excitation line of 532 nm at 10% laser power.

Photoluminescence Spectroscopy. The photoluminescence spectra were collected on an Edinburgh Instruments FS5 fluorescence spectrophotometer. The photoluminescence lifetimes and quantum yields were collected on an Edinburgh Instruments FLS 980 spectrometer.

UV-Vis Absorption Spectra. UV-Vis absorption spectra were recorded using a UV-2600 shimadzu Iadzu UV visible spectrophotometer.

Elemental Analysis. SEM images and EDS data were recorded on a Zeiss Merlin Compact LEO 1530 VP scanning electron microscope. The energy of the electron beam voltage was 10 keV for imaging and was 15 keV for quantitative identifications of elements. Elemental analyses of C, N, and O were performed with a Vario EL Cube.

S1.3 Adsorption Studies

Stable isotope (^{127}I) was used as a surrogate for the radioactive ^{129}I and ^{131}I as their chemical properties are identical.

Iodine Vapour Adsorption Measurement. An open vial (20 mL) containing 20 mg samples was accurately weighted (m_0) and introduced into a glass vessel (150 mL) containing 1 g iodine. The vessel was sealed and kept in an oven at 80 °C. After certain time intervals, the vial containing the sample was weighed periodically (m_t) until the mass of it did not change. The iodine adsorption capacity can be calculated as: $wt\% = (m_t - m_0)/m_0$. Sorption kinetics of iodine by **Th-TCBPA** were fitted to a pseudo first-order kinetics model, $q_t=q_e(1-e^{-kt})$ (where q_t, q_e represent the amounts of adsorbate at certain time t or at equilibrium time, and k is the rate constant) and a pseudo second-order kinetics model, $t/q_t = 1/h + t/q_e$ (where q_t, q_e represent the amounts of adsorbate at certain time t or at equilibrium time, h is the initial adsorption rate, $h = kqe^2$, and k is the rate constant).

S1.4 Luminescence Quenching Study

Finely ground **Th-TCBPA** powder (2 mg) was mixed with 2 mL of $Cr_2O_7^{2-}$ or CrO_4^{2-} solution with various concentrations. The mixture was treated with ultrasonication for 5 min and then stood by for 30 min. The PL spectrum was collected from 400 to 800 nm upon 365 nm UV irradiation on an Edinburgh Instruments FS5 fluorescence spectrometer.

To examine the sensing selectivity toward other cations, 2 mg of finely ground **Th-TCBPA** powder was suspended in 2 mL of 600 mg/kg $M(NO_3)_X$ solution (M = Na^+, Cs^+, Cu^{2+}, Ni^{2+}, Co^{2+}, Al^{3+}, and Fe^{3+}, while X = 1, 2, or 3). To examine the sensing selectivity toward other anions, 2 mg of finely ground Th-TCBPA powder was suspended in 2 mL of 600 mg/kg K_nX solutions (X= F^-, I^-, IO_3^-, ReO_4^-, SO_4^{2-}, CO_3^{2-}, BO_3^{3-}, $Cr_2O_7^{2-}$ and CrO_4^{2-}, n=1, 2 or 3). The PL spectrum of each sample was recorded and that of **Th-TCBPA** in deionized water was collected as a reference to calculate the quenching ratios of anions/cations.

S2. FIGURES AND TABLES

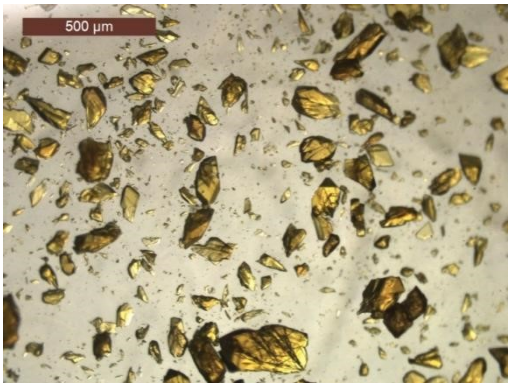

Fig. S1 Crystal image of **Th-TCBPA**.

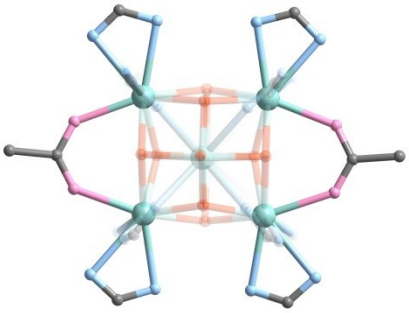

Fig. S2 The schematic diagrams showing the coordination environment of $Th_6(\mu_3\text{-}OH)_8$ SBU in **Th-TCBPA**. Colour code: Th is shown in green, O of μ_3-OH in red, O of CH_3COO^- in pink, and O of $TCBPA^{3-}$ in light blue. Only coordination environments on the equatorial planes are shown and eight $TCBPA^{3-}$ ligands are omitted for clarity.

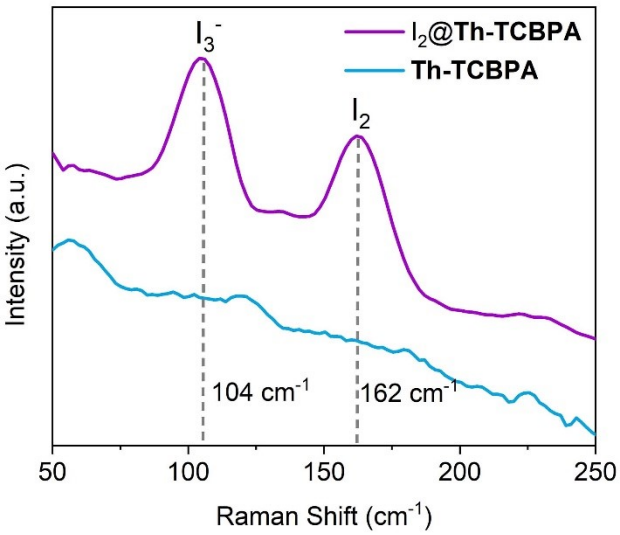

Fig. S3 The Raman spectra of as-synthesized and iodine loaded **Th-TCBPA** samples.

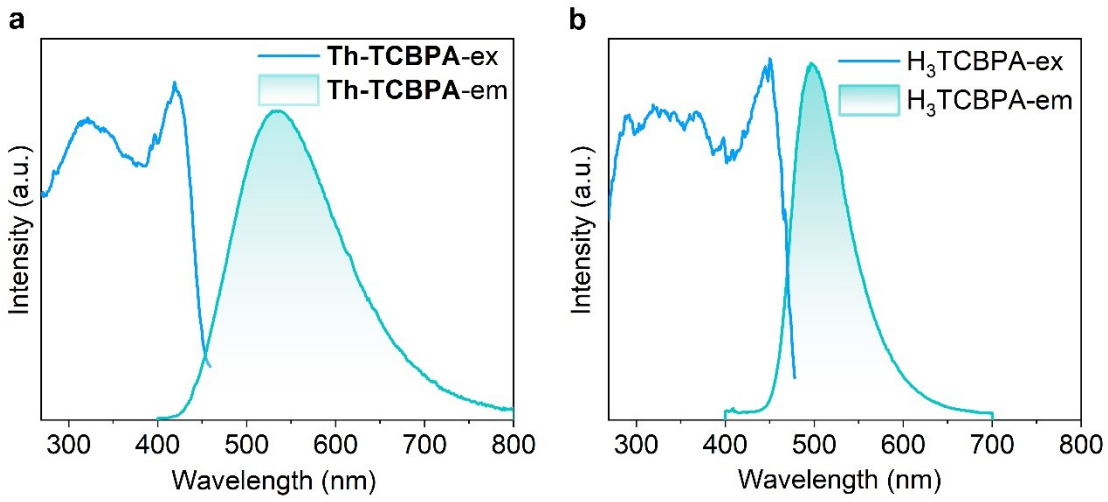

Fig. S4. Excitation and emission spectra of (a) **Th-TCBPA** and (b) H_3TCBPA.

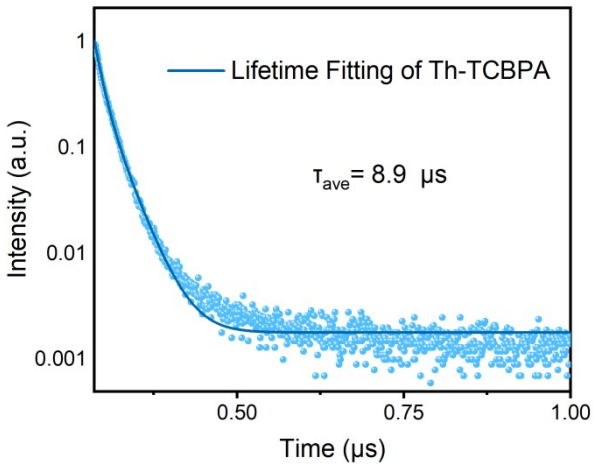

Fig. S5. Photoluminescence lifetime of **Th-TCBPA**.

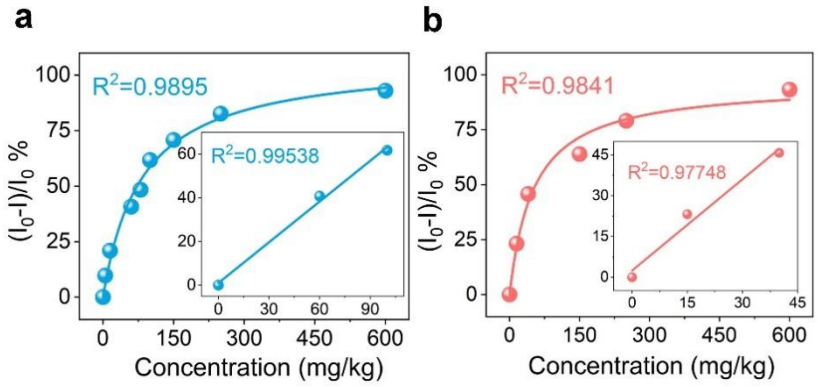

Fig. S6 (a) Correlation between the quenching ratio $(I_0 - I)/I_0$% and CrO_4^{2-} concentration. Inset: linear fit of $(I_0 - I)/I_0$% as a function of CrO_4^{2-} concentration ranging from 0 to 100 mg/kg. (b) Correlation between the quenching ratio $(I_0 - I)/I_0$% and $Cr_2O_7^{2-}$ concentration. Inset: linear fit of $(I_0 - I)/I_0$% as a function of $Cr_2O_7^{2-}$ concentration ranging from 0 to 40 mg/kg.

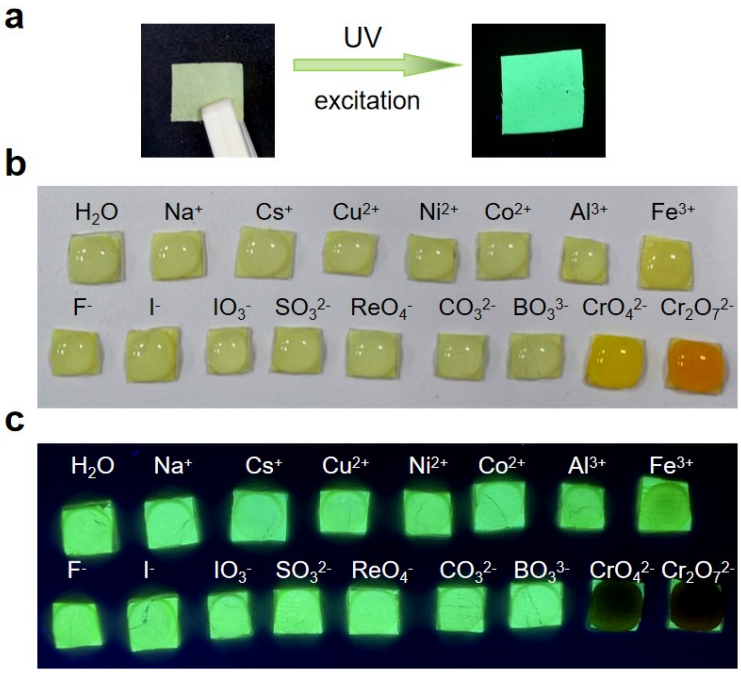

Fig. S7 (a) Photographs of **Th-TCBPA**@PVDF under fluorescence light and upon UV irradiation. (b) The colour of **Th-TCBPA**@PVDF upon contacting with different cations and anions under bright field. (c) Change of the emission colour of **Th-TCBPA**@PVDF upon contacting with different cations and anions.

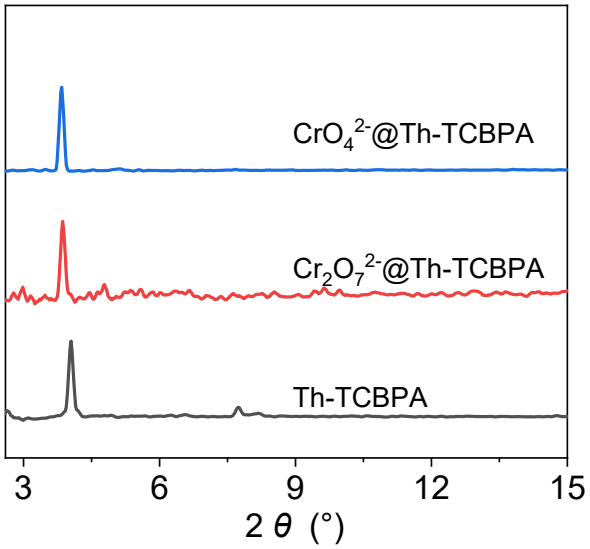

Fig. S8 Powder X-ray diffraction (PXRD) patterns of **Th-TCBPA** before and after being immersed with 600 mg/kg CrO_4^{2-} solution or $Cr_2O_7^{2-}$ solution for 2 hours.

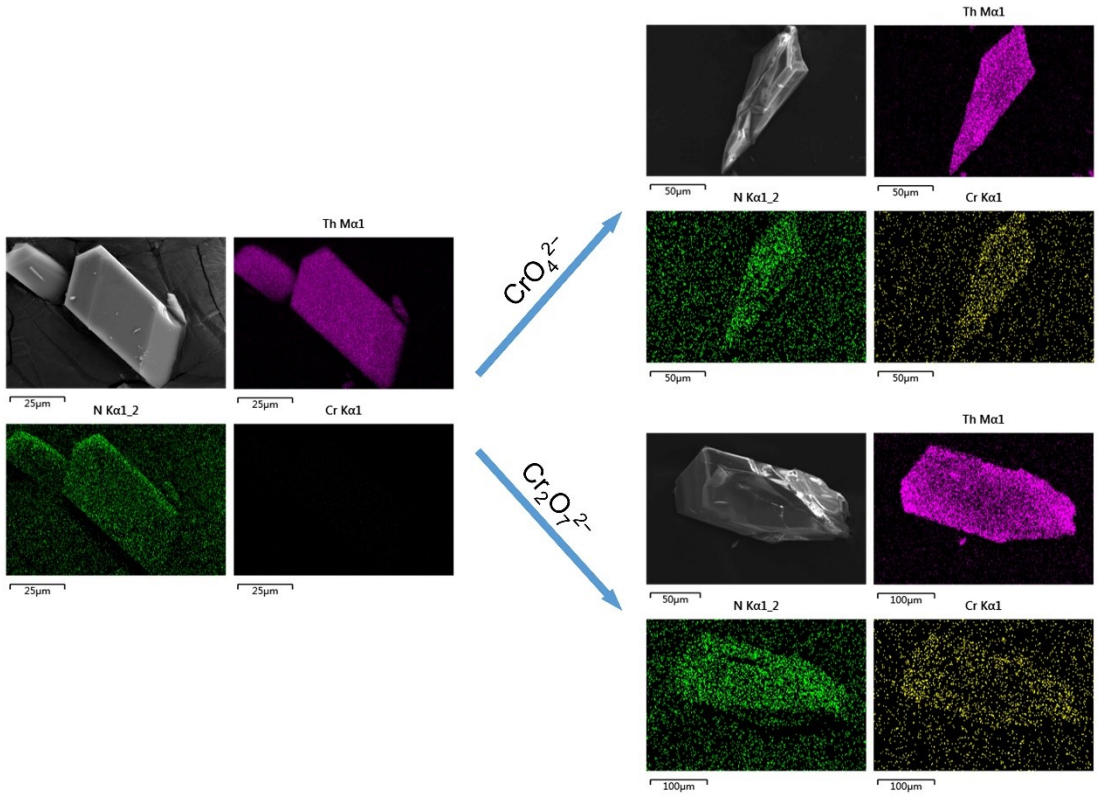

Fig. S9 SEM-EDS mapping of **Th-TCBPA** before and after immersing in CrO_4^{2-} solution and $Cr_2O_7^{2-}$ solution for 2 hours.

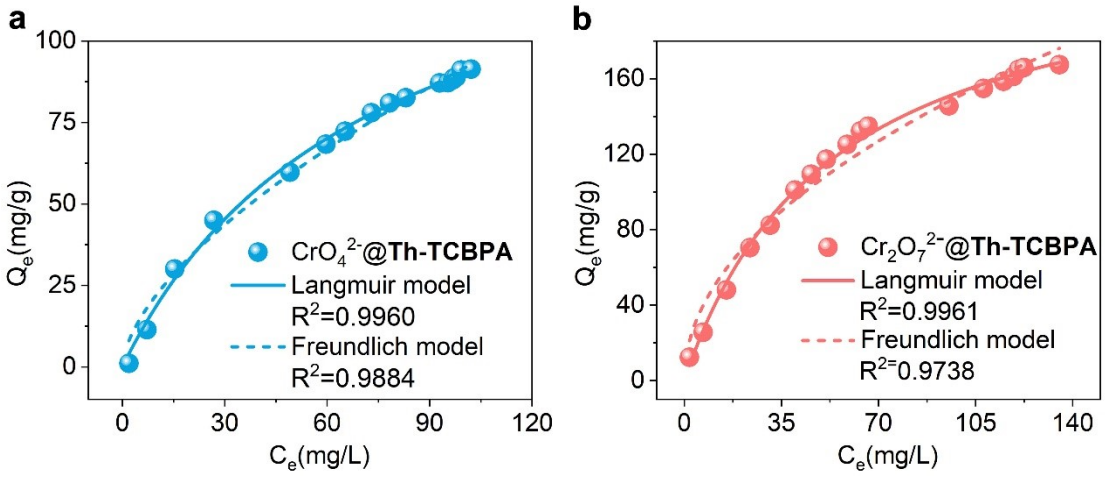

Fig. S10 (a) Sorption isotherms of CrO_4^{2-} by **Th-TCBPA**. (b) Sorption isotherms of $Cr_2O_7^{2-}$ by **Th-TCBPA**.

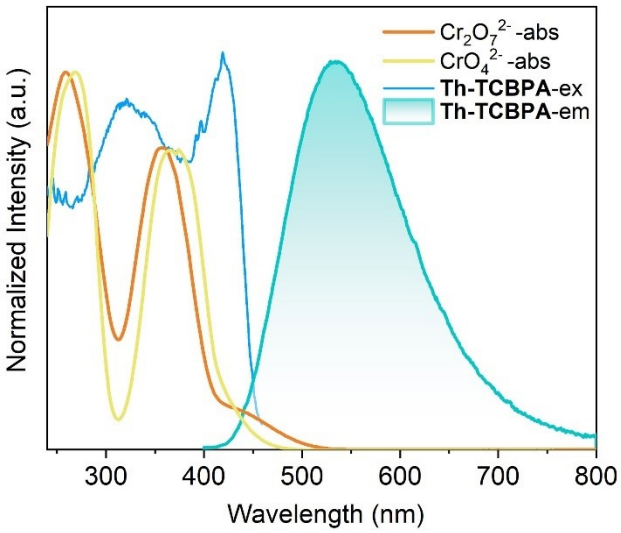

Fig. S11 The absorption spectra of K_2CrO_4 solution and $K_2Cr_2O_7$ solution, as well as the excitation and emission spectra of **Th-TCBPA**.

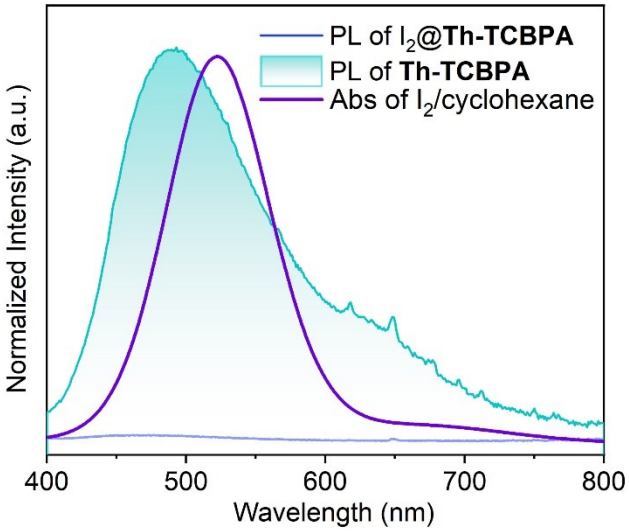

Fig. S12 The absorption spectra of I_2/cyclohexane and emission spectra of **Th-TCBPA**.

Table S1 Crystallographic data for **Th-TCBPA**.

	Code
CCDC number	2216880
Formula	$C_{98}H_{101}N_9O_{32}Th_3$
Formula Weight	2613.03
Habit	block
Space Group	*C*2/*m*
a (Å)	41.8616(9)
b (Å)	26.5661(6)
c (Å)	25.9164(6)
α	90
β	120.8550(10)
γ	90
V (Å^3)	24742.4(10)
Z	8
T (K)	120
λ (Å)	0.71073
Max. 2θ (°)	55.024
ρ_{calcd} (g cm^{-3})	1.403
μ (mm^{-1})	3.667
GoF on F^2	1.062
R_1, wR_2 [I > 2σ(I)]	0.0477, 0.1307
R_1, wR_2 (all data)	0.0703, 0.1405
$(\Delta\rho)_{max}$, $(\Delta\rho)_{min}$/e (Å^{-3})	2.53/-1.63

Table S2 Parameters of the kinetic models for iodine vapor adsorption by **Th-TCBPA**.

pseudo-second-order kinetic model			pseudo-first-order kinetic model		
q_e (mg·g^{-1})	k (g·mg^{-1}·h^{-1})	R^2	q_e (mg·g^{-1})	k (g·mg^{-1}·h^{-1})	R^2
0.5550	1.7946	0.9449	0.8991	0.3890	0.8091

Table S3 Kinetic parameters of the pseudo-second-order model for chromate and dichromate adsorption toward **Th-TCBPA**

	Freundlich model			Langmuir model		
	n	K_F (L^n/mol^{n-1}g)	R^2	Q_m (mg/g)	K_L (L/mg)	R^2
CrO_4^{2-}@**Th-TCBPA**	1.62	5.3(7)	0.9884	155(6)	0.0138	0.9960
$Cr_2O_7^{2-}$@**Th-TCBPA**	2.01	15(2)	0.9738	235(5)	0.0187	0.9961

Table S4 Summary of iodine vapor adsorption in MOFs.

MOFs	Iodine uptake (g/g)
$Ni(44pba)_2$ [6]	1.10
$[Zn_3(DL\text{-}lac)_2(pybz)_2$ [6]	1.01
ZIF-8 [6]	1.25
MFM-300(In, Fe, and Al) [6]	1.16, 1.29, and 0.94
MOF-867 [6]	0.88
UiO-66 [6]	1.17
Th-SINAP-n (n = 7-8)[7]	0.352 and 0.473
Th-SINAP-n (9-15)[8]	0.81, 0.334, 0.43, 0.592, 0.596, 0.358, and 0.7
Th-UiO-66-$(NH_2)_2$ [9]	0.969
Th-TCPBA (this work)	1.01

Table S5 The K_{SV} of selected MOF based sensors for chromate or dichromate.

MOFs	analyte	K_{SV} (M^{-1})
$Cd_2(HDDB)(bib)_{1.5}(H_2O)\cdot 2.5H_2O$ [10]	CrO_4^{2-}	4.70×10^3
	$Cr_2O_7^{2-}$	2.70×10^3
$Cd_2(HDDB)(m\text{-}bimb)]\cdot H_2O$[10]	CrO_4^{2-}	2.50×10^3
	$Cr_2O_7^{2-}$	1.80×10^3
$[Zn_2(mtrb)_2(btec)]\cdot H_2O$ [10]	CrO_4^{2-}	1.62×10^3
	$Cr_2O_7^{2-}$	4.40×10^3
$[Zn_2(tpeb)(bpdc)_2]$ [11]	CrO_4^{2-}	1.085×10^4
	$Cr_2O_7^{2-}$	1.122×10^4
$[Zr_6O_4(OH)_8(H_2O)_4(sbtc)_2]$ (BUT-28) [12]	$Cr_2O_7^{2-}$	1.122×10^5
$Zr_6(OH)_{16}(TBAPy)_2$ (NU-1000) [13]	$Cr_2O_7^{2-}$	1.34×10^4
$Zr_6O_4(OH)_{7(}H_2O)_3(BTBA)_3$ (BUT-39) [14]	$Cr_2O_7^{2-}$	1.57×10^4
Th-TCPBA (this work)	CrO_4^{2-}	$4.4(2)\times10^3$
	$Cr_2O_7^{2}$	$6.6(6)\times10^3$

S3. REFERENCES

1. G. M. Sheldrick, 1996.
2. G. M. Sheldrick, *Acta Crystallographica Section A: Found. Adv.*, 2015, **71**, 3.
3. G. M. Sheldrick, *Acta Crystallogr. Sect. C: Struct. Chem.*, 2015, **71**, 3.
4. O. V. Dolomanov, L. J. Bourhis, R. J. Gildea, J. A. K. Howard and H. Puschmann, *J. Appl. Cryst.*, 2009, **42**, 339.
5. A. L. Spek, *Acta Crystallogr. Sect. C: Struct. Chem.*, 2015, **71**, 9.
6. X. Zhang, J. Maddock, T. M. Nenoff, M. A. Denecke, S. Yang and M. Schröder, *Chem. Soc. Rev.*, 2022, **51**, 3243.
7. Z.-J. Li, Z. Yue, Y. Ju, X. Wu, Y. Ren, S. Wang, Y. Li, Z.-H. Zhang, X. Guo, J. Lin and J.-Q. Wang, *Inorg. Chem.*, 2020, **59**, 4435.
8. Z.-J. Li, Y. Ju, B. Yu, X. Wu, H. Lu, Y. Li, J. Zhou, X. Guo, Z.-H. Zhang, J. Lin, J.-Q. Wang and S. Wang, *Chem. Commun.*, 2020, **56**, 6715.
9. Z.-J. Li, Y. Ju, H. Lu, X. Wu, X. Yu, Y. Li, X. Wu, Z.-H. Zhang, J. Lin, Y. Qian, M.-Y. He and J.-Q. Wang, *Chem. Eur. J.*, 2021, **27**, 1286.
10. B. Parmar, K. K. Bisht, Y. Rachuri and E. Suresh, *Inorg. Chem. Front.*, 2020, **7**, 1082.
11. B. B. Rath and J. J. Vittal, *Inorg. Chem.*, 2020, **59**, 8818.
12. M.-M. Xu, X.-J. Kong, T. He, X.-Q. Wu, L.-H. Xie and J.-R. Li, *Inorg. Chem.*, 2018, **57**, 14260.
13. Z.-J. Lin, H.-Q. Zheng, H.-Y. Zheng, L.-P. Lin, Q. Xin and R. Cao, *Inorg. Chem.*, 2017, **56**, 14178.
14. T. He, Y.-Z. Zhang, X.-J. Kong, J. Yu, X.-L. Lv, Y. Wu, Z.-J. Guo and J.-R. Li, *ACS Appl. Mater. Interfaces*, 2018, **10**, 16650.